NANO LETTERS

Letter

pubs.acs.org/NanoLett

Enhanced Light Emission from Large-Area Monolayer MoS_2 Using Plasmonic Nanodisc Arrays

Serkan Butun,[†] Sefaattin Tongay,[‡] and Koray Aydin*,[†]

[†]Department of Electrical Engineering and Computer Science, Northwestern University, Evanston, Illinois 60208, United States

[‡]School for Engineering of Matter, Transport, and Energy, Arizona State University, Tempe, Arizona 85287, United States

Supporting Information

ABSTRACT: Single-layer direct band gap semiconductors such as transition metal dichalcogenides are quite attractive for a wide range of electronics, photonics, and optoelectronics applications. Their monolayer thickness provides significant advantages in many applications such as field-effect transistors for high-performance electronics, sensor/detector applications, and flexible electronics. However, for optoelectronics and photonics applications, inherent monolayer thickness poses a significant challenge for the interaction of light with the material, which therefore results in poor light emission and absorption behavior. Here, we demonstrate enhanced light emission from large-area monolayer MoS_2 using plasmonic silver nanodisc arrays, where enhanced photoluminescence up to 12-times has been measured. Observed phenomena stem from the fact that plasmonic resonance couples to both excitation and emission fields and thus boosts the light−matter interaction at the nanoscale. Reported results allow us to engineer light−matter interactions in two-dimensional materials and could enable highly efficient photodetectors, sensors, and photovoltaic devices, where photon absorption and emission efficiency highly dictate the device performance.

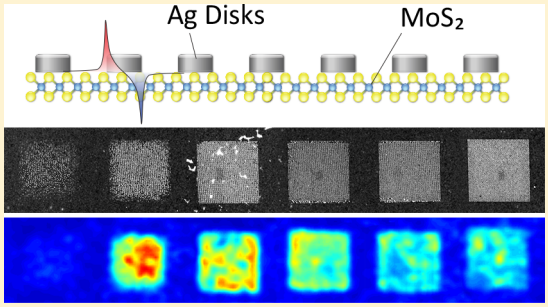

KEYWORDS: *LSPR, 2D materials, MoS_2, photoluminescence, CVD synthesis*

Optical processes such as absorption and emission, particularly in low-dimensional materials such as thin-film semiconductors,[1] graphene,[2−6] carbon nanotubes,[7] nanowires,[8] and organic photovoltaics,[9] can greatly benefit from resonant E-field enhancement using resonant cavities,[10] plasmonics, and photonic crystals.[4] Specifically, plasmonic nanostructures are quite promising for boosting light absorption/emission as they enable very high electric field confinement and are easy to integrate with recently emerging 2D sTMDs. Being a direct band gap semiconductor, monolayer MoS_2 is particularly attractive for a wide range of applications such as field effect transistors,[11−13] sensor/detector applications,[11,14−17] and flexible electronics.[18] Plasmonic materials have been previously shown to facilitate strong light−matter interactions in wide variety of applications and enable enhanced luminescence[19−21] and surface enhanced Raman scattering.[22,23] However, enhanced luminescence demonstrations to date were largely concentrated on single molecules, quantum dots, nanowires, and thin-film semiconductors. Previously, surface plasmon enhanced photocurrent and photoluminescence in MoS_2 was demonstrated by using gold[24] and core−shell[25] nanoparticles. The former was demonstrated on mechanically exfoliated, and the latter was on somewhat small area CVD grown MoS_2 flakes. Moreover, recent developments on growing large area single layer MoS_2 films[26−28] may facilitate them to be used in high-efficiency and low-power light absorbers and emitters. Here, we report on enhanced PL in large area (cm-sized) CVD MoS_2 by coupling these monolayers with designed plasmonic nanoparticle arrays. Large area MoS_2 monolayers allowed us to explore the correlation between the PL emission and the plasmonic resonance of the particles, which was not feasible with smaller area flakes exfoliated directly from MoS_2 crystals. Results show that monolayer PL emission of MoS_2 films is susceptible to E-field intensity variations by LSPR. In addition, we have evidence that not only the excitation field enhancement, but also the emission field scattering enhancement contribute to the overall PL enhancement.

Monolayer CVD MoS_2 samples (Figure 1a) were grown onto 90 nm thermal SiO_2 on bare silicon substrates by high-pressure vapor transport technique (see methods in the Supporting Information). This technique typically yields highly crystalline, continuous, and uniform MoS_2 films as shown in Figure 1, panel a. We confirm that deposited films are indeed monolayers by using three complementary techniques: (1) c-AFM line-scan measurements show that the film thickness measures 0.7 ± 0.1 nm (Figure 1b), which corresponds to reported thickness values for monolayer sTMDs; (2) in-plane (E') and out-of-plane (A^1) Raman modes are separated by ∼18 cm^{-1} (Figure 1c, top panel), which is consistent with the results in literature[16,29,30] owing to indirect to direct gap transition in the quantum confinement limit; and (3) monolayers become highly luminescent with PL peak at ∼670 nm (Figure 1c, bottom panel).

Received: January 30, 2015

DOI: 10.1021/acs.nanolett.5b00407
Nano Lett. XXXX, XXX, XXX−XXX

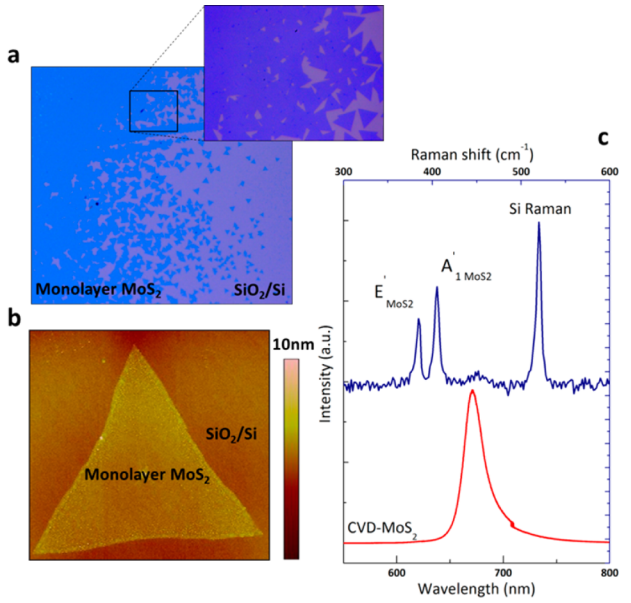

Figure 1. Large area monolayer MoS_2 and diagram of plasmonic heterostructures. (a) Optical images taken on CVD monolayer MoS_2 deposited on 90 nm SiO_2/Si substrates. Dark blue regions (magenta) regions correspond to monolayer MoS_2 (SiO_2/Si) substrates. (b) c-AFM measurements on monolayer MoS_2. (c) micro-Raman (top panel) and micro-PL (bottom panel) measurements taken on the samples. E′ and A'_1 Raman modes are separated by ∼18 cm^{-1}, and monolayers show strong light emission peak at ∼670 nm, which is consistent with the literature values.

After growth, nanodisc arrays with varying diameter (d) sizes were fabricated onto large area monolayer MoS_2 film by conventional e-beam lithography process followed by silver metallization (Figure 2a). Here, varying the diameter of the nanodisc (d) allows us to tune the plasmonic resonance of the nanodisc arrays. For simplicity, we refer this heterostructure as plasmonic/MoS_2 heterostructure in the remaining part of this Letter. In Figure 2, panel b, we show a series of SEM images taken on plasmonic/MoS_2 heterostructures for different d values. As the d value increases from 106 to 227 nm (left to right in Figure 2b), the plasmonic/MoS_2 region becomes brighter under SEM associated with the increased overall Ag coverage on semi-insulating MoS_2 monolayers.

Immediately after the fabrication of nanodisc arrays, we have acquired the spectral PL map of plasmonic array/MoS_2 regions, as shown in Figure 2, panel c. Here, blue and red colors stand for minimum and maximum integrated PL intensity as calculated by integrating measured PL emission from 650−750 nm. Observed spatial variations within each array can be attributed to problems associated with the processing steps such as missing Ag nanodiscs or optical nonuniformity within the MoS_2 monolayer films itself. The enhancement is particularly apparent in the spectral PL emission curves plotted in Figure 2, panel d where each curve is selected at a characteristic maximum point within the plasmonic array. Interestingly, light emission is always greater than pristine monolayers independent from the d values, and the PL peak position remains same, which in return, implies that the dominant excitonic process (i.e., recombination of neutral, charged, or free excitons), to the first order of approximation, can be assumed to be the same for different plasmonic hole array structure parameters.

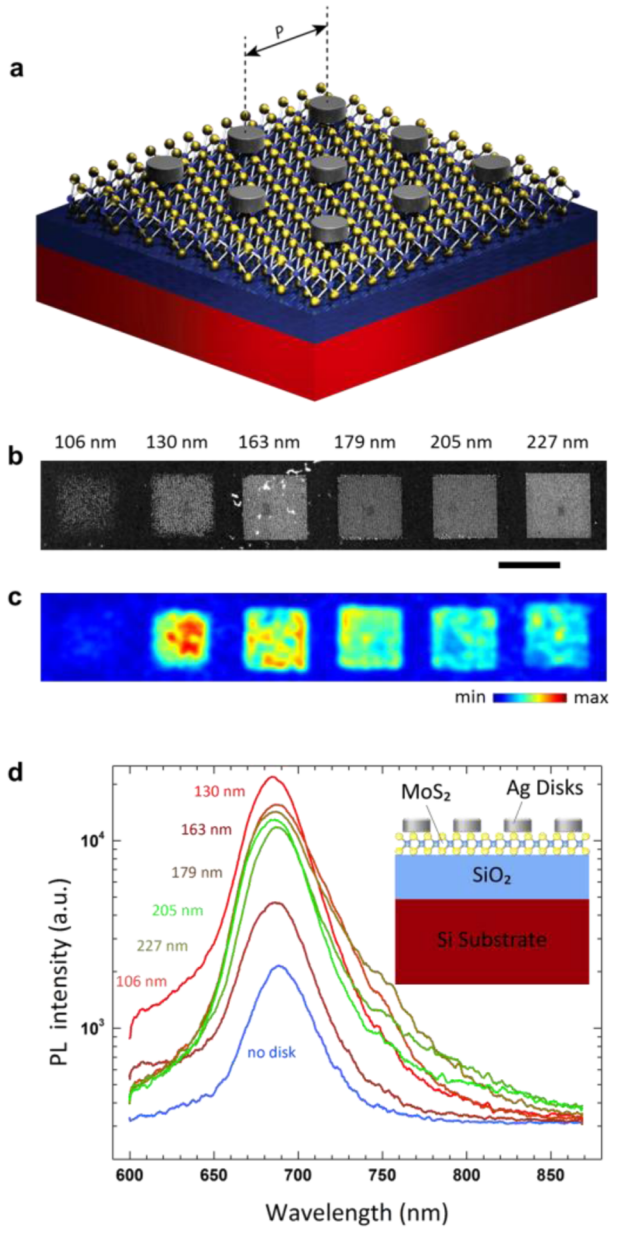

Figure 2. Enhanced PL at plasmonic array/MoS_2 heterostructures. (a) Schematic reporesentation of plasmonic/MoS_2 heterostructures. (b) SEM image of fabricated nanodisc arrays. The diameter of the base unit in each array is indicated above. The scale bar is 25 μm. (c) Corresponding integrated PL map of the area displayed in panel b. (d) PL intensity comparison of selected points in each array. Inset shows the cross-section of the plasmonic/MoS_2 heterostructure.

On the basis of these results, maximum PL emission, which is about 12 times brighter, is achieved only when d is 130 nm, and increasing/decreasing the diameter reduces the emission intensity. The enhancement in PL is calculated by comparing the area under each spectrum in Figure 2, panel d from 650−750 nm. Such diameter-dependent light emission intensity suggests that localized surface plasmon resonance of Ag nanodiscs might be playing critical role in monolayer's optical properties as LSPR highly sensitive to the size of the plasmonic feature. We note that strong emission at 680 nm is evident regardless of the measured position on the array, which corresponds to A1 direct excitonic transition in MoS_2.

DOI: 10.1021/acs.nanolett.5b00407
Nano Lett. XXXX, XXX, XXX−XXX

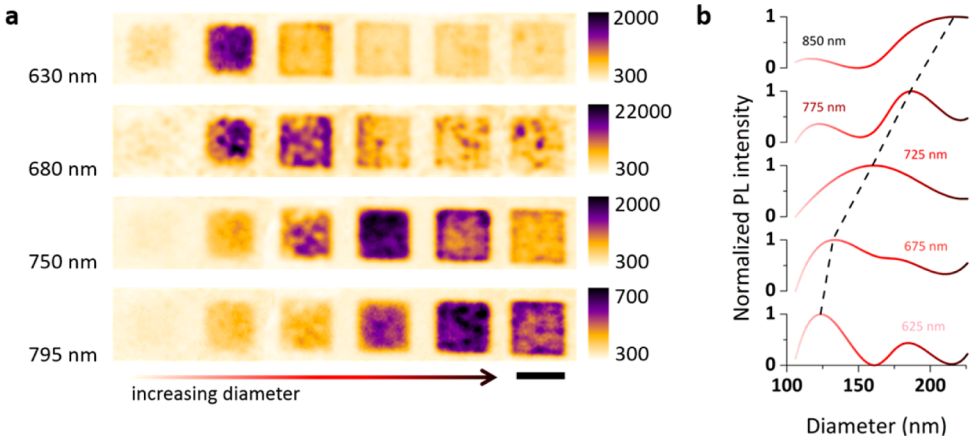

Figure 3. PL emission as a function of Ag nanodisc diameter. (a) PL emission 2D spatial maps at four different wavelengths of six varying diameter nanodisc arrays. Scale bar is 25 μm. Diameters of the discs are 106, 130, 163, 179, 205, and 227 nm from left to right. The periodicity of all arrays is 400 nm. (b) Normalized PL intensity measurements at different wavelengths as a function of diameter. Each curve is normalized within itself. Intermediate diameter points are interpolated using a spline algorithm.

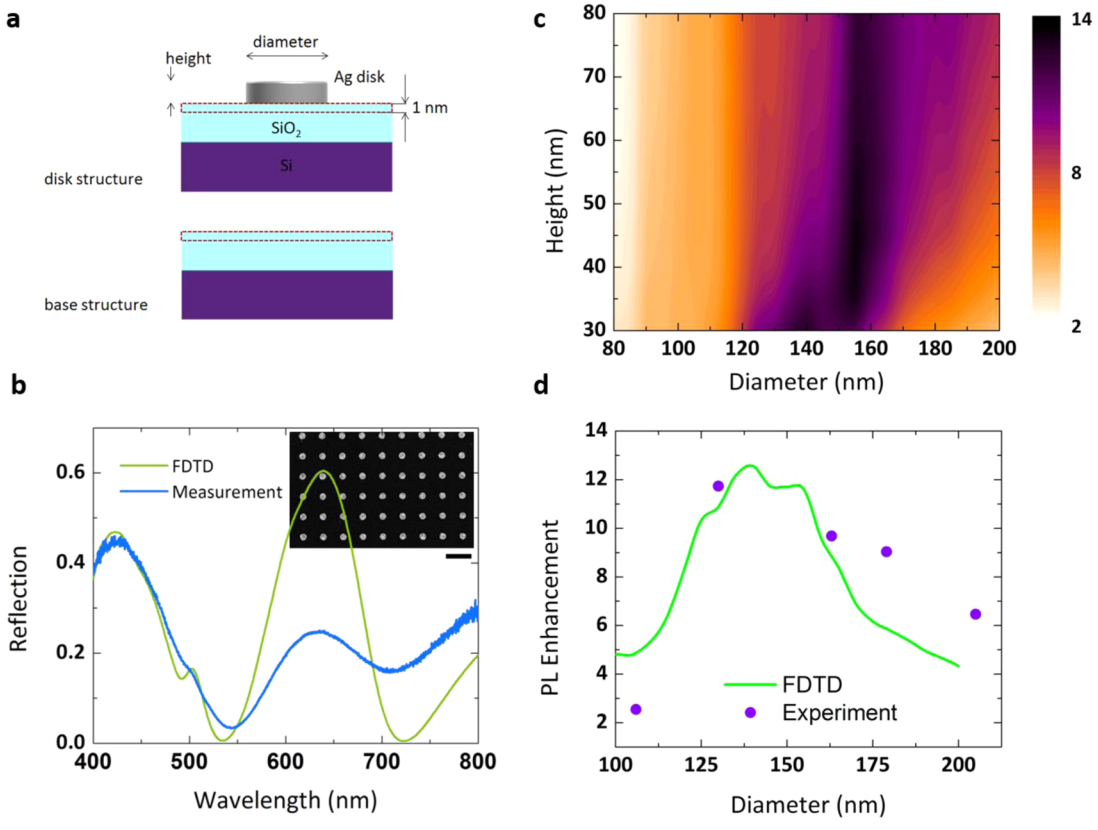

Figure 4. FDTD calculations and experimental comparison (a) Cross-sectional view of the unit cell, which is used in FDTD calculations. Relevant design parameters are indicated. (b) Calculated total E-field enhancement factor in the top 1 nm heighted volume beneath Ag discs. (c) A comparison of measured and calculated reflection curves of a structure of diameter of 130 nm and periodicity of 400 nm. Inset: a SEM image of one of the fabricated Ag disc arrays. The scale bar is 500 nm. (d) A comparison between calculated composite E-field enhancement and measured PL enhancement for nanodiscs of height 50 nm.

To clarify whether the enhancement is due to the excitation field localization around the nanodisc or efficient emission extraction due to scattering at PL emission wavelength, we plotted the PL emission intensity map at different wavelengths (Figure 3a). Interestingly, even though PL intensity is the greatest for d = 130 nm at the PL peak position (680 nm), other arrays with different d values display larger PL intensity at higher wavelengths. For example, at 750 nm, 179 nm diameter array (4th one from left) is brighter compared to other arrays. There is a direct correlation between increasing the d value and wavelength at which the PL intensity enhancement is largest. In addition, the intensity contrast at each wavelength, that is, the difference between the maximum and minimum values of the colorbars next to each PL map in Figure 3, panel a, decreases as the wavelength increases. We attribute this phenomenon to the excitation enhancement. Increasing nanodisc diameter causes a

DOI: 10.1021/acs.nanolett.5b00407
Nano Lett. XXXX, XXX, XXX−XXX

redshift in the plasmonic resonance, which in turn reduces the excitation field to plasmon coupling. As a result, the overall optical excitation of the MoS_2 film decreases.

To elucidate on the emission enhancement as a function of diameter, we have plotted emission counts at specific wavelengths for structures with different diameters in Figure 3, panel b by rearranging the PL data plotted in Figure 2, panel d. Here, PL intensity at each wavelength is plotted as a function of diameter. Missing diameter points are interpolated using a spline algorithm, and each curve is normalized within itself. The dashed line depicts the correlation between the maximum PL emission and the diameter. According to these curves, there is a linear relation between the nanodisc diameter, d, and the wavelength at which the maximum PL emission occurs. That is, for a given wavelength, maximum PL emission takes place over a certain nanodisc diameter. For instance, at 725 nm, maximum PL emission is radiated over 160 nm diameter nanodisc array. This does not mean the maximum PL emission of the entire PL spectrum to be at 725 nm. In fact, the peak emission is still at 680 nm (Figure 2d). However, at 725 nm, maximum emission originates when d = 160 nm. It is well-known that scattering cross-section increases with metallic nanoparticle size, specifically with the diameter in our case. Clearly, increased scattering cross-section of the Ag nanodiscs causes efficient free-space coupling of the PL emission. While these results show evidence for successful emission enhancement, they do not exclude contribution from excitation enhancement.

We have also studied the reflection spectra of Ag nanodisc arrays fabricated directly onto SiO_2/Si substrates. Figure 4, panel a illustrates the methodology that was used for estimating PL enhancement from FDTD calculations. We have calculated the localized E-field intensity upon plane wave excitation in a 1 nm thick volume under the nanodisc. The integrated E-Field intensity as a function of wavelength in this volume is compared to that of a base structure with no nanodisc as shown in Figure 4, panel a. We used the refractive index of SiO_2 for the volume of interest as per the lack of index data of monolayer MoS_2. Assuming equal contribution of E-field intensity enhancement at both excitation and emission wavelengths (543.5 and 680 nm, respectively), the total field enhancement factor, γ_T, can be calculated as follows:

$$\gamma_T = \frac{1}{2}\left(\frac{I_1^{\text{excitation}}}{I_0^{\text{excitation}}} + \frac{I_1^{\text{emission}}}{I_0^{\text{emission}}}\right) \quad (1)$$

where I_x is the integrated E-field intensity calculated over the volume of interest, and subscripts "1" and "0" correspond to conditions with and without nanodiscs, respectively. The thickness of SiO_2 layer is 90 nm, which is the same thickness used in experiments.

We have calculated the enhancement factor as a function of nanodisc diameter and height for a lattice constant (periodicity) of 400 nm. The LSPR resonance of periodic plasmonic nanoparticles is well studied, and it has been shown that the effect of periodicity is rather minor compared to the characteristic size parameters of the nanoparticles provided that interparticle distance is larger than surface plasmon decay length. Therefore, the periodicity of the nanodisc arrays was kept constant in this study. Figure 4, panel c shows the calculated enhancement factor as a function of diameter and height. The maximum enhancement is estimated to be about 13-fold and is a strong function of the diameter. On the other hand, the effect of height is somewhat inferior against the diameter. This is expected as the sample is illuminated normally, only modes along the surface can be excited, which does not depend on material thickness in normal direction provided that it is larger than the skin depth. However, as the height increases, there is an overall enhancement decrease that is attributed to the reduced amount of field penetration into the volume of interest. We have also compared the calculated and the measured reflectivity of similar structures fabricated on Si/SiO_2 substrates without MoS_2 as a function of wavelength. Figure 4, panel b exhibits one such comparison of a structure with d = 130 nm. There is a good agreement between the measurement and FDTD simulation. Intensity mismatch toward the red end of the spectrum can be explained by two factors. The first one is imperfections that arouse during the fabrication process. The second one is related with the measurement set-up. The fact that we are using a high numerical aperture objective limits the amount of light collected. The reduced reflection around excitation wavelength (543.5 nm) and increased reflection around emission wavelength (680 nm) are proof that both emission and excitation enhancement play a role in PL enhancement. Figure 4, panel d plots the estimated PL enhancement against the measured enhancement for a nanodisc array of height 50 nm as a function of diameter. The good agreement further proofs the role of both absorption and scattering of the nanodiscs on PL enhancement.

Understanding the electromagnetic interaction between newly emerging low-dimensional materials with plasmonic structures is crucial for future optoelectronic devices. To investigate this phenomenon, plasmonic nanostructure arrays in close proximity to MoS_2 monolayers were fabricated. With engineered structural parameters, 12-times enhanced PL emission has been observed experimentally. By using systematic analysis, we have proven that PL enhancement reported in this study is both due to the excitation field enhancement at the pump wavelength and efficient scattering at PL emission wavelengths. Efficient light coupling to these low-dimensional materials at nanoscale can break new ground in highly efficient optoelectronic devices such as photodetectors and emitters.

■ ASSOCIATED CONTENT

Supporting Information

Additional information on methods used in this work such as MoS_2 growth, measurements, and FDTD simulations. This material is available free of charge via the Internet at http://pubs.acs.org.

■ AUTHOR INFORMATION

Corresponding Author

*E-mail: aydin@northwestern.edu.

Author Contributions

The manuscript was written through contributions of all authors. All authors have given approval to the final version of the manuscript.

Notes

The authors declare no competing financial interest.

■ ACKNOWLEDGMENTS

This research was supported by the Materials Research Science and Engineering Center (NSF-MRSEC) (DMR-1121262) of Northwestern University. K.A. acknowledges financial support from the McCormick School of Engineering and Applied

DOI: 10.1021/acs.nanolett.5b00407
Nano Lett. XXXX, XXX, XXX−XXX

Sciences at Northwestern University and partial support from the AFOSR under Award No. FA9550-12-1-0280 and the Institute for Sustainability and Energy at Northwestern (ISEN) through ISEN Equipment and Booster Awards. This research made use of the NUANCE Center at Northwestern University, which is supported by NSF-NSEC, NSF-MRSEC, Keck Foundation, and the State of Illinois and the NUFAB cleanroom facility at Northwestern University. S.T. acknowledges Arizona State University Research Seeding Program.

■ ABBREVIATIONS

LSPR, localized surface plasmon resonance; 2D, two-dimensional; CVD, chemical vapor deposition; E-field, electric field; sTMDs, semiconducting transition metal dichalcogenides; PL, photoluminescence; c-AFM, contact mode atomic force microscope; SEM, scanning electron microscopy; FDTD, finite difference time domain

■ REFERENCES

(1) Pryce, I. M.; Koleske, D. D.; Fischer, A. J.; Atwater, H. A. Plasmonic nanoparticle enhanced photocurrent in GaN/InGaN/GaN quantum well solar cells. *Appl. Phys. Lett.* **2010**, *96*, 153501.

(2) Ju, L.; Geng, B.; Horng, J.; Girit, C.; Martin, M.; Hao, Z.; Bechtel, H. A.; Liang, X.; Zettl, A.; Shen, Y. R.; Wang, F. Graphene plasmonics for tunable terahertz metamaterials. *Nat. Nano* **2011**, *6* (10), 630−634.

(3) Thongrattanasiri, S.; Koppens, F. H. L.; García de Abajo, F. J. Complete optical absorption in periodically patterned graphene. *Phys. Rev. Lett.* **2012**, *108* (4), 047401.

(4) Liu, J.-T.; Liu, N.-H.; Li, J.; Li, X. J.; Huang, J.-H. Enhanced absorption of graphene with one-dimensional photonic crystal. *Appl. Phys. Lett.* **2012**, *101*, 052104.

(5) Grigorenko, A.; Polini, M.; Novoselov, K. Graphene plasmonics. *Nat. Photonics* **2012**, *6* (11), 749−758.

(6) Butler, S. Z.; Hollen, S. M.; Cao, L.; Cui, Y.; Gupta, J. A.; Gutierrez, H. R.; Heinz, T. F.; Hong, S. S.; Huang, J.; Ismach, A. F. Progress, challenges, and opportunities in two-dimensional materials beyond graphene. *ACS Nano* **2013**, *7* (4), 2898−2926.

(7) Nikolaenko, A. E.; De Angelis, F.; Boden, S. A.; Papasimakis, N.; Ashburn, P.; Di Fabrizio, E.; Zheludev, N. I. Carbon nanotubes in a photonic metamaterial. *Phys. Rev. Lett.* **2010**, *104* (15), 153902.

(8) Kelzenberg, M. D.; Boettcher, S. W.; Petykiewicz, J. A.; Turner-Evans, D. B.; Putnam, M. C.; Warren, E. L.; Spurgeon, J. M.; Briggs, R. M.; Lewis, N. S.; Atwater, H. A. Enhanced absorption and carrier collection in Si wire arrays for photovoltaic applications. *Nat. Mater.* **2010**, *9* (3), 239−244.

(9) Kang, M.-G.; Xu, T.; Park, H. J.; Luo, X.; Guo, L. J. Efficiency enhancement of organic solar cells using transparent plasmonic Ag nanowire electrodes. *Adv. Mater.* **2010**, *22* (39), 4378−4383.

(10) Sergeant, N. P.; Hadipour, A.; Niesen, B.; Cheyns, D.; Heremans, P.; Peumans, P.; Rand, B. P. Design of transparent anodes for resonant cavity enhanced light harvesting in organic solar cells. *Adv. Mater.* **2012**, *24* (6), 728−732.

(11) Li, H.; Yin, Z.; He, Q.; Li, H.; Huang, X.; Lu, G.; Fam, D. W. H.; Tok, A. I. Y.; Zhang, Q.; Zhang, H. Fabrication of single-and multilayer MoS_2 film-based field-effect transistors for sensing NO at room temperature. *Small* **2012**, *8* (1), 63−67.

(12) Yin, Z.; Li, H.; Li, H.; Jiang, L.; Shi, Y.; Sun, Y.; Lu, G.; Zhang, Q.; Chen, X.; Zhang, H. Single-layer MoS_2 phototransistors. *ACS Nano* **2012**, *6* (1), 74−80.

(13) Radisavljevic, B.; Radenovic, A.; Brivio, J.; Giacometti, V.; Kis, A. Single-layer MoS_2 transistors. *Nat. Nanotechnol.* **2011**, *6* (3), 147−150.

(14) Lopez-Sanchez, O.; Lembke, D.; Kayci, M.; Radenovic, A.; Kis, A. Ultrasensitive photodetectors based on monolayer MoS_2. *Nature Nanotechnol.* **2013**, *8* (7), 497−501.

(15) Lin, J. D.; Han, C.; Wang, F.; Wang, R.; Xiang, D.; Qin, S.; Zhang, X.-A.; Wang, L.; Zhang, H.; Wee, A. T. S.; Chen, W. Electron-doping-enhanced trion formation in monolayer molybdenum disulfide functionalized with cesium carbonate. *ACS Nano* **2014**, *8* (5), 5323−5329.

(16) Nan, H.; Wang, Z.; Wang, W.; Liang, Z.; Lu, Y.; Chen, Q.; He, D.; Tan, P.; Miao, F.; Wang, X.; Wang, J.; Ni, Z. Strong photoluminescence enhancement of MoS_2 through defect engineering and oxygen bonding. *ACS Nano* **2014**, *8* (6), 5738−5745.

(17) Tongay, S.; Zhou, J.; Ataca, C.; Liu, J.; Kang, J. S.; Matthews, T. S.; You, L.; Li, J.; Grossman, J. C.; Wu, J. Broad-range modulation of light emission in two-dimensional semiconductors by molecular physisorption gating. *Nano Lett.* **2013**, *13* (6), 2831−2836.

(18) Bertolazzi, S.; Brivio, J.; Kis, A. Stretching and breaking of ultrathin MoS_2. *ACS Nano* **2011**, *5* (12), 9703−9709.

(19) Kinkhabwala, A.; Yu, Z.; Fan, S.; Avlasevich, Y.; Mullen, K.; Moerner, W. E. Large single-molecule fluorescence enhancements produced by a bowtie nanoantenna. *Nat. Photonics* **2009**, *3* (11), 654−657.

(20) Biteen, J. S.; Lewis, N. S.; Atwater, H. A.; Mertens, H.; Polman, A. Spectral tuning of plasmon-enhanced silicon quantum dot luminescence. *Appl. Phys. Lett.* **2006**, *88*, 131109.

(21) Tanaka, K.; Plum, E.; Ou, J. Y.; Uchino, T.; Zheludev, N. I. Multifold enhancement of quantum dot luminescence in plasmonic metamaterials. *Phys. Rev. Lett.* **2010**, *105* (22), 227403.

(22) Willets, K. A.; Van Duyne, R. P. Localized surface plasmon resonance spectroscopy and sensing. *Annu. Rev. Phys. Chem.* **2007**, *58*, 267−297.

(23) Cinel, N. A.; Bütün, S.; Ertaş, G.; Özbay, E. "Fairy chimney"-shaped tandem metamaterials as double resonance SERS substrates. *Small* **2013**, *9* (4), 531−537.

(24) Lin, J.; Li, H.; Zhang, H.; Chen, W. Plasmonic enhancement of photocurrent in MoS_2 field-effect transistor. *Appl. Phys. Lett.* **2013**, *102*, 203109.

(25) Sobhani, A.; Lauchner, A.; Najmaei, S.; Ayala-Orozco, C.; Wen, F.; Lou, J.; Halas, N. J. Enhancing the photocurrent and photoluminescence of single crystal monolayer MoS_2 with resonant plasmonic nanoshells. *Appl. Phys. Lett.* **2014**, *104*, 031112.

(26) Zhan, Y.; Liu, Z.; Najmaei, S.; Ajayan, P. M.; Lou, J. Large-area vapor-phase growth and characterization of MoS_2 atomic layers on a SiO_2 substrate. *Small* **2012**, *8* (7), 966−971.

(27) Liu, K.-K.; Zhang, W.; Lee, Y.-H.; Lin, Y.-C.; Chang, M.-T.; Su, C.-Y.; Chang, C.-S.; Li, H.; Shi, Y.; Zhang, H.; Lai, C.-S.; Li, L.-J. Growth of large-area and highly crystalline MoS_2 thin layers on insulating substrates. *Nano Lett.* **2012**, *12* (3), 1538−1544.

(28) Lee, Y. H.; Zhang, X. Q.; Zhang, W.; Chang, M. T.; Lin, C. T.; Chang, K. D.; Yu, Y. C.; Wang, J. T. W.; Chang, C. S.; Li, L. J. Synthesis of large-area MoS_2 atomic layers with chemical vapor deposition. *Adv. Mater.* **2012**, *24* (17), 2320−2325.

(29) Lee, C.; Yan, H.; Brus, L. E.; Heinz, T. F.; Hone, J.; Ryu, S. Anomalous lattice vibrations of single- and few-layer MoS_2. *ACS Nano* **2010**, *4* (5), 2695−2700.

(30) Splendiani, A.; Sun, L.; Zhang, Y.; Li, T.; Kim, J.; Chim, C.-Y.; Galli, G.; Wang, F. Emerging photoluminescence in monolayer MoS_2. *Nano Lett.* **2010**, *10* (4), 1271−1275.

DOI: 10.1021/acs.nanolett.5b00407
Nano Lett. XXXX, XXX, XXX−XXX